Physics of Stimulated $L \rightarrow H$ Transitions

K. Miki,[1] P. H. Diamond,[1,2] S.-H. Hahn,[3] W. W. Xiao,[1] Ö. D. Gürcan,[4] and G. R. Tynan[2]

[1]*WCI Center for Fusion Theory, National Fusion Research Institute, Daejeon 305-333, Republic of Korea*
[2]*CMTFO, University of California, San Diego, California 92093, USA*
[3]*KSTAR Team, National Fusion Research Institute, Daejeon 305-333, Republic of Korea*
[4]*LPP, Ecole Polytechnique, CNRS, 92118 Palaiseau Cedex, France*

We report on model studies of stimulated $L \rightarrow H$ transitions. These studies use a novel reduced mesoscale model. Studies reveal that $L \rightarrow H$ transitions can be triggered by particle injection into a subcritical state (i.e., $P < P_{\mathrm{Thresh}}$). Particle injection alters the edge mean flow shear via changes of density and temperature gradients. The change of edge mean flow shear is critical to turbulence collapse and the subsequent stimulated transition. For low ambient heating, strong injection is predicted to trigger a transient turbulence collapse. We predict that repetitive injection can maintain the turbulence collapse and so sustain a driven H-mode-like state. The total number of particles required to induce a transition by either injection or gas puffing is estimated. Results indicate that the total number of injected particles required is much smaller than that required for inducing a transition by gas puffing. Thus, we show that internal injection is more efficient than gas puffing of comparable strength. We also observe that zonal flows do not play a critical role in stimulated transitions.

Bifurcations between different system states are ubiquitous in the physics of nonlinear systems. Examples include, but are not limited to, the transition from overturning cells to global circulation in Rayleigh-Bénard convection [1], first and second order phase transition fronts [2,3], nonlinear waves in excitable media [4], etc. The class of state bifurcations includes transport bifurcations in confined plasmas, in which the system transitions from a turbulent state of strong anomalous transport, to a regime of good confinement. A prime example of such a transition is the well known $L \rightarrow H$ transition [5]. The H mode has now become "standard operating procedure" for tokamak plasmas with good confinement [6]. Thus, it is the regime anticipated for ITER operation, and is thought to be critical to ignition and burning plasma operation. The $L \rightarrow H$ transition requires sufficient heating, fueling and torque so as to trigger the formation of an edge transport barrier, which is effectively a thermal insulation layer supported by a strongly sheared $E \times B$ flow [7]. The sheared flow is thought to self-organize by a process of multistate evolution involving zonal flow (ZF) amplification, cyclic oscillations, and eventual "locking in" of a stage of suppressed turbulence by strong diamagnetic $E \times B$ shear [8–12]. The $L \rightarrow H$ transition has a well defined separatrix heat flux threshold for which the empirical trends have been extensively studied [13,14].

The critical role of the H mode in the ignition of a burning plasma has motivated an extensive research effort aimed at achieving control of the $L \rightarrow H$ transition and the associated $H \rightarrow L$ back transition and hysteresis [15]. As a first step toward control, considerable effort has been expended at understanding (qualitatively and

quantitatively) the sequence of ZF and mean flow (MF) evolution which occurs during the $L \rightarrow H$ transition [12,16]. Results indicate that above a certain threshold, Reynolds work of the turbulence on the ZF depletes the turbulence energy to the point of collapse. Transport is, thus, drastically reduced. As a consequence, heating and fueling drive a rapid increase in ∇p_i, generating strong diamagnetic $E \times B$ shear which signals the onset of the H phase. The physics of this multistep process ultimately sets the $L \rightarrow H$ threshold. A quantitative model of the threshold power scaling is developing, but is not yet complete [12,14,17].

Control of the $L \rightarrow H$ transition and the $H \rightarrow L$ back transition is desirable, on account of the tight margin for the ITER power threshold and the uncertainty in hysteresis for ITER. Progress from understanding to achieving control has been limited. Research work on control has focused mainly on fueling by strongly pulsed gas puffing or by supersonic molecular beam injection (SMBI) as means to improve on standard gas fueling by more effectively optimizing (i.e., increasing) the near edge electric field shear $\langle V_E \rangle'$. Experimental results [18–20] indicate that (i) intense puffing and pellet injection can trigger transitions, sometimes at substantially subcritical powers, and (ii) the key element in these transitions seems to be a rapid change in the edge electric field shear, which is induced by injection. In particular, injection methods or procedures which do not significantly change edge $\langle V_E \rangle'$ seemingly do not induce transitions. In this Letter, we discuss very significant progress in understanding a class of "stimulated" $L \rightarrow H$ transitions, which occur for $P < P_{\mathrm{Th}}$. In particular, we present the discovery of a transient

H-mode state, which can be maintained by repetitive injection. More generally, this Letter elucidates the role of fueling in the $L \rightarrow H$ transition and sheds new light on the role of zonal flows in the bifurcation process. We present a testable prediction of the relative timing of zonal flow Reynolds work and mean flow shearing in both spontaneous and stimulated transitions. Such relative timing reveals much about the mechanism of the transition.

We have developed a five-field (turbulence intensity, mean square ZF shear, ion pressure p, and density n, profiles and mean poloidal mass flow), two-predator—one-prey model of the $L \rightarrow H$ transition [12] which incorporates a particle source related to internal fueling, and the associated cooling process enforced by pressure balance. To address the effect of pellets, SMBI, etc., we include additional fueling $\delta\Gamma_{n,\mathrm{SMBI}}$ and $\delta\Gamma_{p,\mathrm{SMBI}}$ in the density and pressure equation. The density equation change due to pellet injection or SMBI is

$$\delta\Gamma_{n,\mathrm{SMBI}} = \frac{I_{\mathrm{SMBI}}(n_{\mathrm{ref}})}{\tau_{\mathrm{SMBI}}} \sum_i \frac{1}{2}[H(t - t_i)$$
$$- H(t - t_i - \tau_{\mathrm{SMBI}})]\exp\left(-\frac{(a - x_{\mathrm{dep}})^2}{2\Delta x^2}\right).$$

Here, the important parameters characterizing particle injection are I_{SMBI}: the strength of particle injection proportional to the total number of particle injection, τ_{SMBI}: the duration of particle injection, x_{dep}: the deposition depth, and Δx: the width of deposition, (all are illustrated in Fig. 1). $H(t)$ is Heaviside function. $n_{\mathrm{ref}} = 0.11$ is a coefficient, referring to the density at $r/a = 0.975$ [See Fig. 2(d)]. Reference values for these factors are $x_{\mathrm{dep}} = 0.975(r/a)$, $\Delta x = 0.02(r/a)$, $\tau_{\mathrm{SMBI}} = 250(a/c_s)$, $I_{\mathrm{SMBI}} = 10$–50. These parameters are consistent with realistic values from SMBI experiments [21].

For the pressure perturbation, we note $\delta\Gamma_{p,\mathrm{SMBI}} \sim 0$ on times long compared to the acoustic time scale $\tau > R/c_s$, due to pressure balance. We assume that sound waves will relax the SMBI-induced pressure perturbation quickly on the time scale R/c_s. Note also that the identity $p = nT$ implies cooling due to particle injection, i.e.,
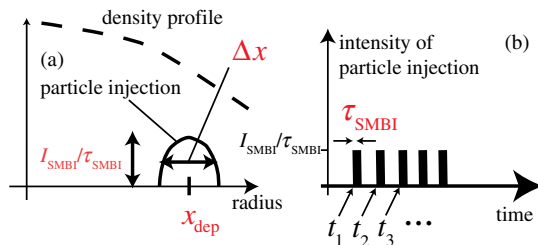
$\delta\Gamma_{T,\mathrm{SMBI}} = -(T_{\mathrm{ref}}/n_{\mathrm{ref}})\delta\Gamma_{n,\mathrm{SMBI}}$. Thus, the temperature decreases due to particle injection, on account of $\delta p \sim 0$.

We model time dependent gas puffing from an edge source by adding the new term $\delta\Gamma_{n,\mathrm{gp}}$ to the density equation, i.e., $\delta\Gamma_{n,\mathrm{gp}} = \delta\Gamma_a \partial_r\{\exp[-((a - r + d_a)^2/(2L_{\mathrm{dep}}^2))]\}(1/2)[H(t - t_i) - H(t - t_i - \tau_{\mathrm{gp}})]$. We assume that gas puffing uniformly modulates fueling effects, thus neglecting source poloidal and toroidal asymmetry. The fueling source $\Gamma_a + \delta\Gamma_a$, replaces Γ_a, during the time τ_{gp}, where Γ_a represents the fueling source in the density evolution. The duration of gas puffing is assumed to be longer than that of particle injection. $\tau_{\mathrm{SMBI}} = 250(a/c_s) \sim 1$ msec and $\tau_{\mathrm{gp}} = 3000(a/c_s) \sim 10$ msec is chosen to be consistent with experiments [18,21].

Keep in mind that there are many limitations of this reduced model. Regarding injection, there is no treatment of the ablation and ionization process. Injection is modeled as instantaneous, so the time delay related to ionization, etc., is not accurately represented. We do not consider toroidal and poloidal source asymmetry. Also, the model does not evolve toroidal rotation V_ϕ, and so does not account for possible benefits from reduction in rotation due to injection. In future work, we will include edge electron temperature effects on scrape-off-layer heat transport [17], and treat lower-single-null vs upper-single-null asymmetry [22].

Results for the case in Fig. 2 show that particle injection triggers a subcritical $L \rightarrow H$ transition. We set a moderate intensity of injection, with shallow deposition. These parameters are consistent with those from SMBI experiments [21]. Heating is subcritical ($dQ(\equiv (Q_{\mathrm{crit}} - Q)/Q_{\mathrm{crit}}) = 0.5$),
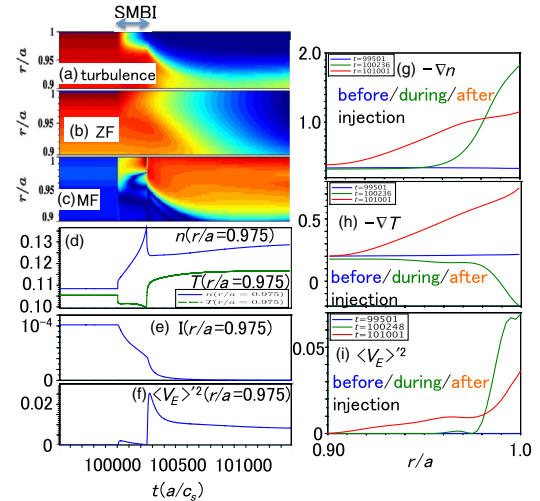

FIG. 1 (color online). Illustrations of particle injection, (a) showing the deposition structure, with the location of deposition x_{dep}, the width of deposition Δx, and the intensity of particle injection I_{SMBI}; (b) showing the time evolution of particle injection. The duration of particle injection is τ_{SMBI}.

FIG. 2 (color online). Results for model calculation, (I_{SMBI}, τ_{SMBI}, x_{dep}/a, $\Delta x/a$, dQ) = (30, 250(a/c_s), 0.975, 0.02, 0.5). Particle injection occurs during $t = 100\,000 - 100\,250(a/c_s)$. (a)–(c) Spatiotemporal evolution of turbulence intensity, ZF, and MF, respectively. Evolution of (d) density and temperature, (e) turbulence intensity I, and (f) MF shear $\langle V_E \rangle'^2$, at $r/a = 0.975$, respectively. (g), (h), (i) Profiles of $-\nabla n$, $-\nabla T$, and $\langle V_E \rangle'^2$ before (blue), during (green), after (red) injection.

so the system is in L mode, and no limit-cycle oscillation appears. Here, Q is the ambient heat flux and Q_{crit} is the critical heat flux threshold for which the $L \rightarrow H$ transition occurs spontaneously. In Figs. 2(a)–2(c), the $L \rightarrow H$ transition is triggered by the immediate collapse of edge turbulence upon injection, and the region of turbulence collapse then expands inward. The excitation of MF shear follows the turbulence collapse after injection. MF shear locks in H mode. Due to particle injection, density increases and temperature decreases, as seen in Fig. 2(d). In Figs. 2(g) and 2(h), the density gradient peaks at the edge during injection, and the temperature profile flattens locally there. After injection, both the temperature and density gradients remain peaked at the edge. Turbulence is quickly quenched following injection in Fig. 2(e). After injection, a single rapid burst in $\langle V_E \rangle'^2$ [in Fig. 2(f)] is followed by its relaxation to the H phase value, with enhanced edge $\langle V_E \rangle'$ in Fig. 2(i). Fueling induces transitions by driving the edge $\langle V_E \rangle'$ sufficiently to exceed the threshold for quenching turbulence. We find that deeper injection does not trigger the $L \rightarrow H$ transition, but instead triggers a damped oscillation. There, edge turbulence is not completely quenched after injection, but recovers during a damped oscillation of turbulence, ZF, and MF. A key difference from the previous case is that the edge $\langle V_E \rangle'$ was not enhanced.

Next, we address the question concerning the relative merits of gas puffing and SMBI. In particular, we aim to elucidate precisely how much better SMBI is for triggering transitions than gas puffing is. Here, we introduce quantitative comparisons of the total number of particles necessary to trigger $L \rightarrow H$ transition by SMBI with that using gas puffing. This comparison is a basic measure of the relative efficiency of the two fueling methods. We estimate the total number of particles introduced by gas puffing. Using $\Gamma_a = 10^{-4}(c_s/a)$, the critical intensity of gas puffing $\delta\Gamma_a/\Gamma_a = 3.6$, and $\tau_{gp} = 3000(a/c_s)$, we find the total number of particles introduced by gas puffing to be $\Delta N_{gp} = 1.08$. We now compare the number of particles added by gas puffing to that added by particle injection, by examining the case of particle injection with edge deposition, $x_{dep} = 1.0$. Using the critical intensity of injection $I_{SMBI} = 30$, we obtain $\Delta N_{SMBI} = 0.083$. The comparison of ΔN_{gp} and ΔN_{SMBI} indicates that particle injection triggers the transition with much fewer particles than gas puffing does. The large difference between the total number of particles indicates that injection causes a large change in edge profiles and $\langle V_E \rangle'$, which is essential for the transition. Short, intense particle pulsation can more easily induce $\langle V_E \rangle'$ changes with a smaller total number of particles. The lesson we learned here is that intense and rapid particle injection inside the separatrix, as opposed to slow gas puffing, is optimal for transition.

We find that injection into a subcritical state can trigger a transient turbulence collapse for a lower ambient heating power $dQ \sim 0.7$. Once the system enters the transient H mode, weak heating does not sustain a MF shear sufficient to quench the turbulence. The turbulence then advances or spreads from the core into the quiescent edge region, as observed in the $H \rightarrow L$ back transition [15,23]. We discover that sequential, repetitive injection into a subcritical state can sustain the turbulence collapse, as shown in Fig. 3. This sustainment of turbulence collapse may be thought of as a "driven H mode." Through the repetitive, sequential injection, edge $\langle V_E \rangle'$ exhibits continuous enhancement. By subsequent injection before the system returns to the L mode, the system can maintain the stimulated H-mode-like state. We find that stronger I_{SMBI} results in a longer transient H mode. Thus, the important factors which determine the "driven H-mode" state are I_{SMBI}, dQ, and the frequency of sequential particle injection f_{SMBI}.

We now explore the fundamentals of the trigger mechanism for the transitions, with special emphasis on ZFs. In Fig. 2(b), there is no evidence of a ZF burst prior to, or at the transition. Rather, the edge $\langle V_E \rangle'$ indeed seems to be a key to the stimulated transition. However, without any external source or noise, and with increasing heat flux, the $L \rightarrow H$ transition spontaneously evolves via the
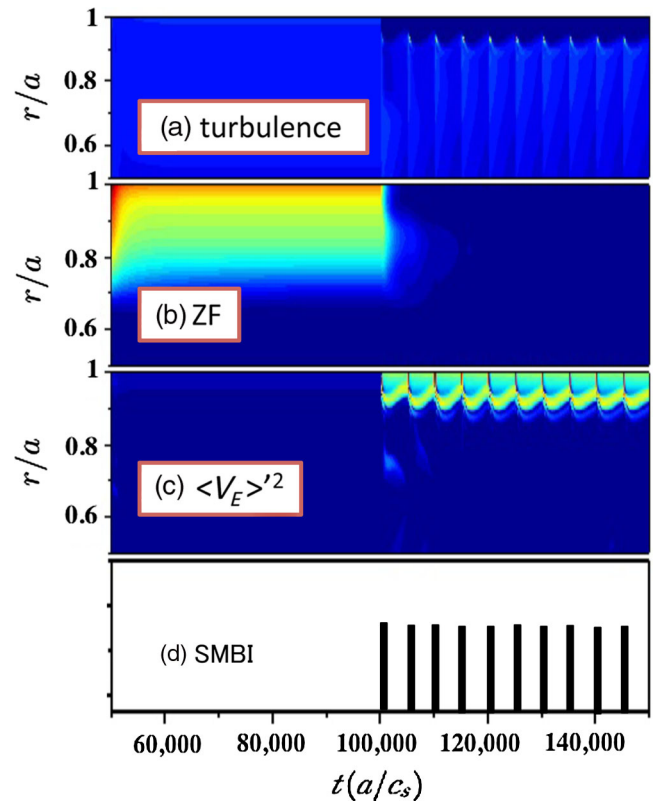

FIG. 3 (color online). Results of model calculation, ($t_i = 100000 + 5000i(a/c_s)$ ($i = 0, 1, \ldots$) (i.e., sequential shots), (I_{SMBI}, $\tau_{SMBI}, x_{dep}/a, \Delta x/a, dQ$) = $(50, 250(a/c_s), 0.975, 0.02, 0.7)$.): (a)–(c) spatiotemporal evolution of turbulence intensity, ZF, and MF, respectively. Repetitive, sequential particle injection sustains edge $\langle V_E \rangle'$, thus H mode maintains.

mediation of ZF, which appears to play a central role [12]. There, the ZF acts as a "holding pattern" in which to store increasing fluctuation energy without increasing transport, thus allowing the MF shear to increase and lock in the transition. In particular, in the spontaneous transition, a peak in the normalized Reynolds work of the turbulence on the ZF has been shown to precede the transition [16]. Given the contrast between the findings for spontaneous and stimulated transitions, further study and clarification are required.

Based on the predator-prey model, we explore the roles of ZF and MF in the two kinds of transitions by introducing the following parameters [12,16]: $R_T = \alpha_0 E_0/(\gamma_L - \Delta\omega I)$, and $R_H = \alpha_V E_V/(\gamma_L - \Delta\omega I)$. Here, R_T measures the rate of energy transfer from turbulence into ZF, normalized by the rate of energy input into the turbulence. When R_T exceeds order unity, the turbulence can collapse, allowing rapid steepening of ∇p. Turbulence collapse occurs due to coupling of fluctuation energy to the ZF. R_H is the rate of shearing of the turbulence by the MF, normalized by the energy input into the turbulence. When R_H exceeds order unity, turbulence is quenched by MF shearing, leading to locking in of the H mode. We track R_T and R_H evolution in both the spontaneous and stimulated transitions.

For the case of the spontaneous transition [Fig. 4(a)], the peak of R_T at $r/a = 1.0$ [at time (A)] clearly precedes the peak in R_H at $r/a = 1.0$ [at time (B)]. This sequence suggests a causal relation between ZF and MF at the edge. In contrast, for the case of the stimulated transition [Fig. 4(b)], the peaks of R_T and R_H coincide. This result suggests that the ZF coupling is not critical for stimulated transitions and that there is no causal link between ZFs and MFs in such transitions. We note, then, that the spontaneous and stimulated transitions take fundamentally different routes to achieve transport and profile bifurcation.

To summarize, we have elucidated several key aspects of the physics of stimulated $L \rightarrow H$ transitions, and compared the evolution of these to those of spontaneous transitions. A reduced $L \rightarrow H$ transition model has been developed to explore the effect of internal deposition. By using internal deposition, we can achieve stimulated transitions for lower ambient heating than we achieve spontaneous transitions for. Particle injection, i.e., internal fueling near the edge, can trigger a subcritical $L \rightarrow H$ transition. The key effect caused by injection is a change of edge MF shear $\delta\langle V_E\rangle'$ induced by changes of density and temperature gradients. The density gradient peaks at the edge during injection, while the temperature profile softens at the edge. Edge mean shear $\langle V_E\rangle'$ is shown to be critical to turbulence collapse and the injection-induced transition. The injection-induced transition is sensitive to the number of particles injected per unit time, the location of deposition, and the degree of heating below the threshold. Strong injection triggers a transient subcritical turbulence
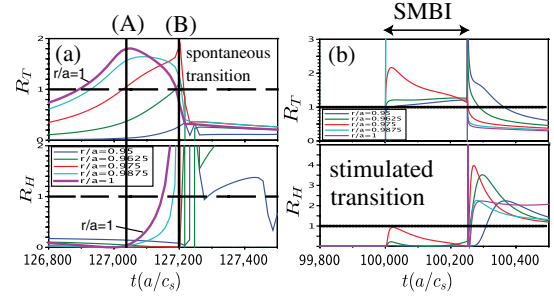

FIG. 4 (color online). Temporal evolution of R_T and R_H, at various radial locations $r/a = 0.95, 0.9625, 0.975, 0.9875, 1.0$ for the case of (a) spontaneous, and (b) stimulated $L \rightarrow H$ transitions.

collapse. Repetitive injection at a period less than the lifetime of the collapsed state can maintain the subcritically collapsed state, leading to a driven, or "stimulated" H mode. The total number of particles required to induce a transition by either injection or gas puffing is estimated. The total number of injected particles is shown to be significantly smaller than that added by gas puffing. A change in edge profiles and $\langle V_E\rangle'$ is seen to be critical to the transition—i.e., internal injection is more effective than gas puffing of comparable strength, for triggering transitions. Bursty or oscillatory behavior of ZFs is not evident for injection-induced transition. Peaks in time of R_T and R_H coincide in the case of stimulated transitions, suggesting there is no causal link between ZFs and MFs for injection-induced transitions. This is in contrast to spontaneous transitions.

Naturally, we ask how these results fit into our understanding of the $L \rightarrow H$ transition. This finding suggests that there can be multiple pathways to the transition and that not all such pathways involve the same mechanism. So, how do we reconcile the apparent difference in the evolution of stimulated and spontaneous transitions? Both transitions consist of heating and fueling, but are quite different in the distributions of heating and fueling. The stimulated transition and spontaneous transitions take fundamentally different routes to achieve transport and profile bifurcations. The spontaneous transition achieves the transition via ZF excitation, to reduce turbulence and then steepen ∇p_i. The external injection of the stimulated transition directly steepens edge $\langle V_E\rangle'$ and ∇p_i. Though these routes to transition look different, increased edge $\langle V_E\rangle'$ locks in to the H mode in both cases. The difference between the two transitions lies in how the state enhanced by edge $\langle V_E\rangle'$ is achieved. More generally, there are studies that elucidate the differences in mechanism between spontaneous and externally stimulated transition mechanisms.

[1] H. Mori and Y. Kuramoto, *Dissipative Structures and Chaos* (Springer-Verlag, Berlin, 1998).

[2] R. A. Fisher, Ann. Eugenics **7**, 355 (1937).

[3] A. Kolmogorov, I. Petrovsky, and N. Piscounoff, Bull. Moskov Gos. Univ. **A1**, 1 (1937).

[4] B. P. Belousov, in *Oscillations and Traveling Waves in Chemical Systems*, edited by R. Field and M. Burger (John Wiley, New York, 1985), pp. 605–613.

[5] F. Wagner, G. Becker, K. Behringer, D. Campbell, A. Eberhagen *et al.*, Phys. Rev. Lett. **49**, 1408 (1982).

[6] C. Gormezano, A. C. C. Sips, T. C. Luce, S. Ide, A. Becoulet, X. Litaudon *et al.*, Nucl. Fusion **47**, S285 (2007).

[7] P. H. Diamond, S.-I. Itoh, K. Itoh, and T. S. Hahm, Plasma Phys. Controlled Fusion **47**, R35 (2005).

[8] T. Estrada, T. Happel, C. Hidalgo, E. Ascasibar, and E. Blanco, Europhys. Lett. **92**, 35 001 (2010).

[9] G. S. Xu, B. N. Wan, H. Q. Wang, H. Y. Guo, H. L. Zhao *et al.*, Phys. Rev. Lett. **107**, 125001 (2011).

[10] L. Schmitz, L. Zeng, T. L. Rhodes, J. C. Hillesheim, E. J. Doyle, R. J. Groebner, W. A. Peebles, K. H. Burrell, and G. Wang, Phys. Rev. Lett. **108**, 155002 (2012).

[11] T. Estrada, C. Hidalgo, T. Happel, and P. H. Diamond, Phys. Rev. Lett. **107**, 245004 (2011).

[12] K. Miki, P. H. Diamond, Ö. D. Gürcan, G. R. Tynan, T. Estrada, L. Schmitz, and G. S. Xu, Phys. Plasmas **19**, 092306 (2012).

[13] Y. R. Martin and T. Takizuka (the ITPA CDBM *H*-mode Threshold Database Working Group), J. Phys. Conf. Ser. **123**, 012033 (2008).

[14] F. Ryter, T. Pütterich, M. Reich, A. Scarabosio, E. Wolfrum, R. Fischer *et al.*, Nucl. Fusion **49**, 062003 (2009).

[15] K. Miki, P. Diamond *et al.* (to be published).

[16] P. Manz, G. S. Xu, B. N. Wan, H. Q. Wang, H. Y. Guo *et al.*, Phys. Plasmas **19**, 072311 (2012).

[17] W. Fundamenski, F. Militello, D. Moulton, and D. McDonald, Nucl. Fusion **52**, 062003 (2012).

[18] L. G. Askinazi, V. E. Golant, S. V. Lebedev, L. S. Levin, V. A. Rozhansky, and M. Tendler, Phys. Fluids B **5**, 2420 (1993).

[19] P. Gohil, L. R. Baylor, T. C. Jernigan, K. H. Burrell, and T. N. Carlstrom, Phys. Rev. Lett. **86**, 644 (2001).

[20] X. R. Duan, J. Q. Dong, L. W. Yan, X. T. Ding, Q. W. Yang *et al.*, Nucl. Fusion **50**, 095011 (2010).

[21] W. W. Xiao, P. H. Diamond, X. L. Zou, J. Q. Dong, X. T. Ding *et al.*, Nucl. Fusion **52**, 114027 (2012).

[22] N. Fedorczak, P. Diamond, G. Tynan, and P. Manz, Nucl. Fusion **52**, 103013 (2012).

[23] T. Estrada, C. Hidalgo, and T. Happel, Nucl. Fusion **51**, 032001 (2011).